STATUS OF A TWO-PHASE CFD APPROACH TO THE PTS ISSUE

P. Coste[1], J. Pouvreau[1], J. Laviéville[2], M. Boucker[2]

[1]Commissariat à l'Energie Atomique, Grenoble, FRANCE. pierre.coste@cea.fr
[2]Electricité de France, Chatou, FRANCE.

Abstract

A two-phase CFD modelling approach of the Pressurized Thermal Shock (PTS) problem has been developed and is being validated in the context of PWR life time safety studies. The cold water injection results in strong condensation and complex 3D two-phase phenomena. Direct Contact Condensation (DCC) occurs on the jet and on the free surface of the stratified flow in the leg. These surfaces are much larger than the cells size used in the computational domain, in this sense they can be called large interfaces. DCC depends strongly on the liquid side heat transfer, which is modelled as a function of turbulence, which itself depends on momentum exchange between gas and liquid. A statistical model is used to represent turbulence in each phase. The large interfaces require a special modelling. It has been recently developed and implemented in the NEPTUNE_CFD code which is based on an Eulerian two-fluid model. The present status of this large interface modelling is presented. The validation relies on separate effects experiments such as air-water or steam-water stratified flows and on a more integral experiment, COSI, which represents a cold leg scaled 1/100 for volume and power from a PWR under SBLOCA conditions. The interest of the considered experimental data for PTS CFD is discussed.

1 INTRODUCTION

In the context of PWR life time safety studies, it is important to evaluate the mechanical constraints on the reactor pressure vessel during some postulated accidental scenarios. The Pressurized Thermal Shock (PTS) is one of these. During a postulated Loss Of Coolant Accident (LOCA), as the pressure can still be high in the system, typically between 2 and 7 MPa, cold water is injected from emergency core cooling systems into the cold leg. It flows toward the downcomer, inducing thermal constraints on the vessel due to the temperature rapid decrease. Estimating this water temperature is the so-called PTS problem from the thermohydraulics point of view.

Since two decades, it is possible to evaluate such a temperature with system codes (Janicot, 1993), but it is an averaged value in the cross section of the cold leg. It is obvious that CFD allows to get rid of such an assumption but it is just as much obvious that CFD gives rise to serious difficulties, as listed in the Lucas *et al.* (2007) review. The flow during a PTS is composed of a turbulent free liquid jet impacting the free surface of the turbulent horizontal stratified flow in the cold leg, submitted to a turbulent vapour flow. The liquid temperature depends strongly on Direct Contact Condensation (DCC) which takes place on the free surfaces and which interacts with the complex transient three dimensional dynamic conditions.

Given the complexity involved by a CFD approach, a first option followed by Coste (2004) was to directly tackle the integral problem, starting from the COSI experiment which represents a cold leg scaled 1/100 for volume and power from a PWR under SBLOCA conditions, in order to range and start to quantify the most important phenomena. A second option followed by Yao *et al.* (2005) was to start from each individual model (turbulence, friction, DCC) and to validate each of them on separate effects experiments. Roughly speaking, the shortcoming was that models developed in the first option did not give satisfactory results on separate effects experiments and models developed in the second option did not give satisfactory results on COSI. The objective of our studies is to tackle this shortcoming; the objective of this paper is to give the present status of those studies.

The paper is organised as follows. In the first part, the choice of the two-fluid model and the basic equations are briefly discussed. In the next parts, each model used in present PTS related studies is

outlined. Then validation calculations in which each model is involved are presented. The relevance of each experiment with respect to CFD validation for PTS is discussed.

2 BASIC EQUATIONS AND CODE FRAMEWORK

2.1 Choice of the two-phase model

Direct Numerical Simulations (DNS), for example Nagasoa (1999) or Fulgosi *et al.* (2003), are useful to learn about large scale structures close to the free surface and detailed statistics of the dynamic and scalar fields but they remain confined to low Reynolds numbers. Large Eddy Simulations (LES) allow the study of situations with higher Reynolds numbers (Magnaudet and Calmet, 2006). Liovic and Lakehal (2007) used an LES/VOF combination to calculate the case of air/steam injection into a water pool. Such techniques based on one-velocity field are promising. However, aiming at calculating the reactor case or integral experiments in parallel with model developments since the beginning of the studies in the early 2000's, CFD codes based on the two-fluid model were selected to address the problem from the CFD angle because of their generality and their intrinsic ability to treat heat and mass transfers at large scales and any Reynolds numbers.

2.2 Equations solved by NEPTUNE_CFD in PTS related calculations

The six classical transport equations (mass, momentum and energy for both liquid and gas) of the two-phase model, with the same pressure in the two phases, as established for example in Ishii (1975), are solved by the NEPTUNE_CFD code (Méchitoua *et al.* (2003), Guelfi *et al.* (2007)). The NEPTUNE_CFD solver is based on a pressure correction fractional step approach. The discretization follows a 3D full unstructured finite volume approach, with a collocated arrangement of all variables. Numerical consistency and precision for diffusive and advective fluxes for nonorthogonal and irregular cells are taken into account through a gradient reconstruction technique. Convective schemes for all variables, except pressure, are centered/upwind scheme. Velocities components can be computed with a full centered scheme. Gradients are calculated at second order for regular cells and at first order for highly irregular cells. The time step is variable with a CFL condition equal to unity.

3 INTERFACIAL AREA

3.1 Large Interface modelling

The two-phase model resulting from averaging process leads to specific problems in case of flows with free surfaces like stratified flow or liquid jet in steam. Specific closures are needed. Within the framework of CFD based on the two-phase model, such flows lead to configuration of interfaces larger than cells size, called afterward Large Interfaces (LI's). In this case, closure laws for friction, heat transfer or turbulence are different inside the LI regions and outside. It is then necessary to locate the LI's position at each time step of the simulation in order to apply the correct closure laws. Our approach differs from approaches which aim at simulating the LI's location in the context of one momentum equation, like Volume Of Fluid, level set or front tracking, in that it only locates the position, it does not reconstruct it. In the calculations of this paper, the surface tension is not taken into account on LI's.

The interface detection method implemented in NEPTUNE_CFD is based on the gradient of liquid fraction (Coste *et al.*, 2008). The first step consists in computing a *refined liquid fraction gradient*, based on harmonic or anti-harmonic interpolated values of liquid fraction on the faces between the cells (Laviéville and Coste, 2008). This refined gradient allows to detect the cells belonging to the LI, in two steps, corresponding to two criteria.

First step: each component of the refined gradient is compared with a maximum value based on the mesh geometry. The cells in which at least one component verifies Eq. (1) are selected (criterion C_1).

$$\left.\frac{\partial \alpha_L}{\partial x_i}\right)_{refined} > C_1 \left.\frac{\partial \alpha_L}{\partial x_i}\right)_{geometry} \quad (1)$$

Second step: the interface is refined in order to get only one cell in the LI's normal direction. When two neighbouring cells selected in the first step make a line between them which is not *normal enough to the interface* (criterion C_2, Eq. (2)), one of these two cells is removed from the interface: the one with the lowest liquid fraction.

$$\left|\left(\nabla_{refined}\alpha_L^I + \nabla_{refined}\alpha_L^J\right).\underline{IJ}\right| > C_2 \left\|\nabla_{refined}\alpha_L^I + \nabla_{refined}\alpha_L^J\right\| \left\|\underline{IJ}\right\| \quad (2)$$

The combination of both criteria, with the heuristically determined values 0.2 for C_1 and 0.7 for C_2, allows to detect the interface with a correct precision in many conditions. This method for sure has some shortcomings in some flow configurations but it has been used satisfactorily in the PTS context.

The specific LI's closure laws developed and implemented in NEPTUNE_CFD code (Coste *et al.*, 2007, 2008) use not only the cell of the LI but also the two neighbouring ones located in LI's normal direction, on both sides, liquid and vapour: these models consider a wide interface of three cells, called afterward LI3C. It allows to use only physically relevant values by choosing the interface side where the phase is not residual. Closure laws are based on three cells instead of only one, so it limits the effect of the LI's position with regard to the meshing. The detection of the neighbouring cells corresponding to the LI's ones is made by selecting cells (in liquid and vapour) in the direction of the normal of the interface, given by the gradient of liquid fraction. When the interface is smeared, several LI3C may overlap. In this case, the LI3C with the lowest gradient is removed.

3.2 Test case

The LI3C detection has been tested on several 3D configurations with large interface. A simple 2D test case is illustrated in Fig. 1: the liquid is on the left at the initial time and then it sloshes under the influence of gravity. The calculated LI3C at time 0.2 s is plotted, where blue cells are stratified cells, green cells are the liquid neighbouring cells and yellow cells are the neighbouring vapour cells. A few cells pointed out by arrows have been removed from the LI3C by the algorithm due to the overlap of LI3C.

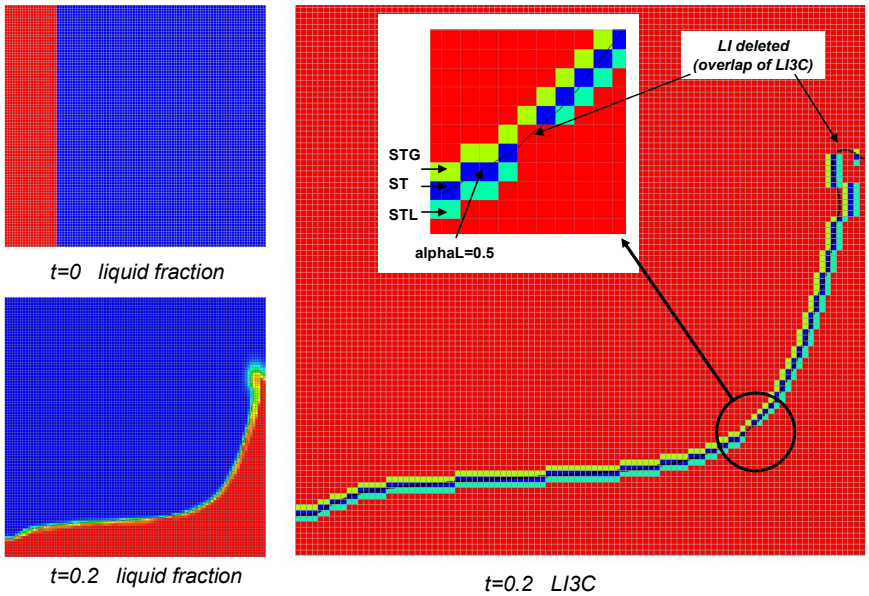

Fig. 1. NEPTUNE_CFD calculation of a 2D test case for three-cells-thick large interface detection. Left: liquid fractions from 1 (red) to zero (blue). Right: regular cells (red) and three cells thick large interface (green, navy blue and sky blue).

4 TURBULENCE AND FRICTION

4.1 Friction Model

An anisotropic two-phase friction is assumed close to free surfaces. This is because the friction of bubbles with liquid, in the case of bubbles coming up to a free horizontal stratified flow surface, for example, is completely different from the friction of the gas over the free surface, which sees the liquid rather like a wall. Then the drag coefficient F_p^{LG} between liquid (*L)* and gas (*G*) phases, in the *p* direction defined in Fig. 2, is a general two-phase one derived from droplet and bubble drags, as was done in the SIMMER-III code (Tobita *et al.*, 2006). The drag coefficient in the *LI* plane (index o, Fig. 2), F_o^{LG}, is specific to large interfaces. The basic hypothesis of the present model is that the free surface is a wall for the gas, a wall moving at the interface velocity u_{int}. The i component of the friction is then written as follows:

$$J'_{\tau(L\to G),i} = -\alpha_L \left(F_o^{LG}\, u_{r,o,i}^{LG} + F_p^{LG}\, u_{r,p,i}^{LG} \right) \tag{3a}$$

where the relative velocity between phases *L* and *G* is:

$$\vec{u}_r{}^{L,G} = \vec{u}_G - \vec{u}_L \tag{3b}$$

The wall law of Van Driest (1956) is used to calculate F_o^{LG}, in which the *LI* is replacing the wall:

$$u^+ = \int_0^{y+} \frac{2\, d\xi}{1 + \sqrt{1 + 4\kappa^2 \left(1 - \exp(-\xi / A)\right)^2 \xi^2}} \tag{4}$$

where $\kappa = 0.42$ and A=25.6. The output of the wall law on the *q* phase side is a friction velocity u_q^*. The inputs of the wall law are, in the *LI* case, -a- the modulus of the relative velocity between the *LI* and the *q* phase taken at a distance which is characteristic of the discretization, $u_{\tau,q}$, -b- the distance between the *LI* and the point where this relative velocity is taken. $u_{\tau,q}$ calculation requires an hypothesis to calculate u_{int}. In Coste *et al.* (2007) calculations performed on the basis of NEPTUNE_CFD V1.0.6, the hypothesis was that u_{int} was equal to the liquid velocity of the STL cell. In other words, the difference of velocity between the liquid in STL cell and u_{int} was neglected. In NEPTUNE_CFD V1.0.7, this difference is calculated with the hypothesis according to which the tangential shear on gas side is equal to the shear on liquid side:

$$\rho_L\, u_{\tau,L}^{*\,2} = \rho_G\, u_{\tau,G}^{*\,2} \tag{5}$$

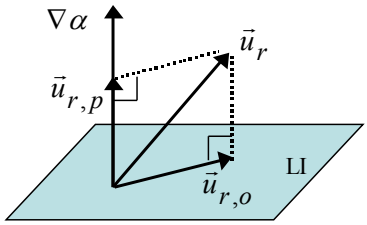

Fig. 2. Projections of the relative velocity (index r) on the direction parallel (index p) to the normal of the large interface (LI) and on the LI which is a plane orthogonal (index o) to the p direction.

4.2 Turbulence model

The Reynolds stress tensor is closed with a Boussinesq-like assumption. A two-equation k-ε model for the calculation of the turbulent eddy viscosity is used: one for each phase in the whole domain. It is an extension to multi-phase flows of the classical model used in single phase flows. The decrease of turbulence due to thermal stratification is included. It is a non negligible effect as was shown in a first simple CFD of COSI tests (Coste, 2004). Turbulence production due to the influence of each phase on the other one depends along the LIs on the interfacial friction. There is no model for turbulence damping at the free surface.

4.3 Validation on an air-water stratified flow

We consider an experiment featuring an adiabatic air water co-current stratified flow, in a 12 m long, 20 cm wide, 10 cm high, 0.1% slope rectangular channel (Fabre *et al.*, 1987). The inlet liquid superficial velocity is 0.15 m/s. Our selected test cases in this paper are runs 250 and 400. The inlet gas superficial velocity of run 250, 2.5 m/s, is high enough for the interfacial friction to play an important role, and sufficiently weak for waves and 3D circulations to be negligible. The inlet gas superficial velocity of run 400, 4.0 m/s, is high enough for waves and 3D circulations. The water height is 3.8 cm (resp. 3.15) in run 250 (resp. 400). The measurements used for the CFD comparisons are done 9.1 m from the inlet. These are vertical profiles of volume fraction, average velocities and turbulence quantities, in liquid and gas.

Calculations are performed with the NEPTUNE_CFD code. The base case mesh used in the calculations is 2D, uniform, structured and rectangular, with 50 cells in the length and 20 in the height. The three directions are (*x,y,z*): x is the channel axis, axial, y is the height, z is the third direction. The comparisons between calculations and experiment are in Fig. 3 and Fig. 4. The most important parameters from the PTS point of view are horizontal average velocities u_x *(horiz. velocity)* and k *(turb. kin. energy)* on liquid (*liq.*) side ($u_{L,x}$, k_L), in particular close to the free surface. On the gas side close to the free surface, the average horizontal velocity $u_{G,x}$ is important because it has a strong effect on the interfacial friction, which in turn has an effect on k_L close to the surface. The measured liquid and gas turbulent shear stresses, respectively $\left\langle u'_{L,x}u'_{L,y}\right\rangle$ and $\left\langle u'_{G,x}u'_{G,y}\right\rangle$, where u' are turbulent velocity fluctuations, have an almost linear profile in the smooth case.

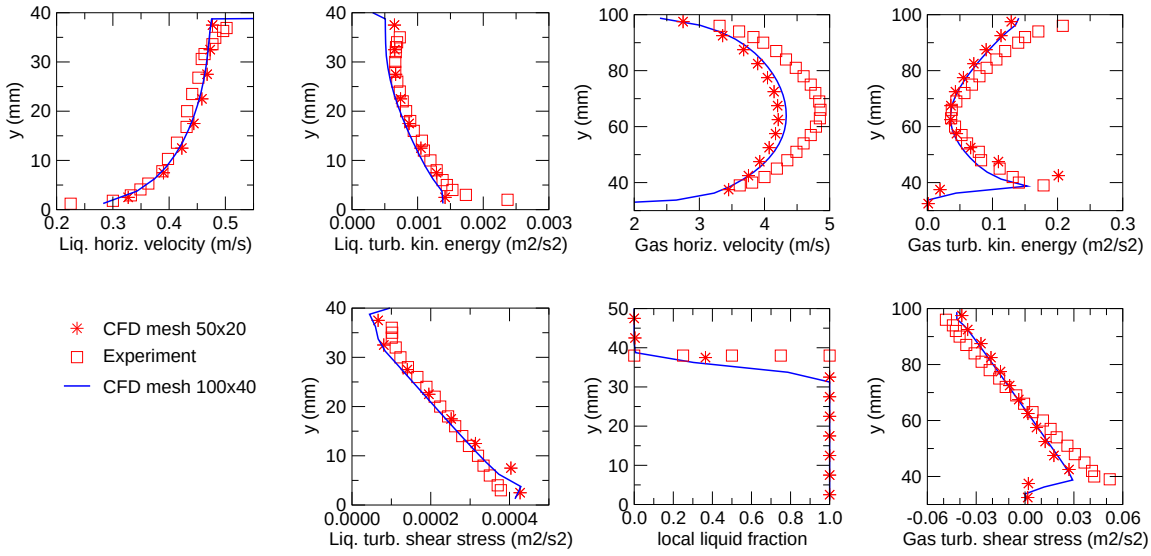

Fig. 3. Run 250 (smooth) - NEPTUNE_CFD Calculation with large interface turbulence and friction models with the base case mesh (✳) (2D, 50x20 cells) and with two times smaller cells (—) (2D, 100x40) versus measurements (□), 9.1 m from the inlet.

Fig. 3 shows calculations of Run 250 (smooth free surface). Details about these calculations can be found in Coste *et al.* (2007). They are done both with the base case mesh and with a refined mesh with two times smaller cells in the two space directions. The calculated liquid axial horizontal velocity profile does not have the measured S-like shape due to the liquid entrainment by the gas just below the free surface: a feature of the flow is missing. The liquid turbulent shear stress close to the wall and close to the free surface has some discrepancies with the measurements. However the agreement and the weak sensitivity to the mesh refinement are satisfactory for a CFD use in PTS, at the present stage.

Fig. 4 shows NEPTUNE_CFD calculations of run 400, a run with a wavy free surface. They are done both with the base case mesh (2D, 50x20) and with a 3D mesh (50x20x20). The discrepancy between 2D and 3D calculation is large. The plots of liquid horizontal velocity and liquid turbulent shear stresses rule out the 2D calculations of wavy runs such as this run 400. The calculation finds the decrease of the water level between the runs 250 and 400 but it is unable to correctly predict the run 400 profiles especially in the gas.

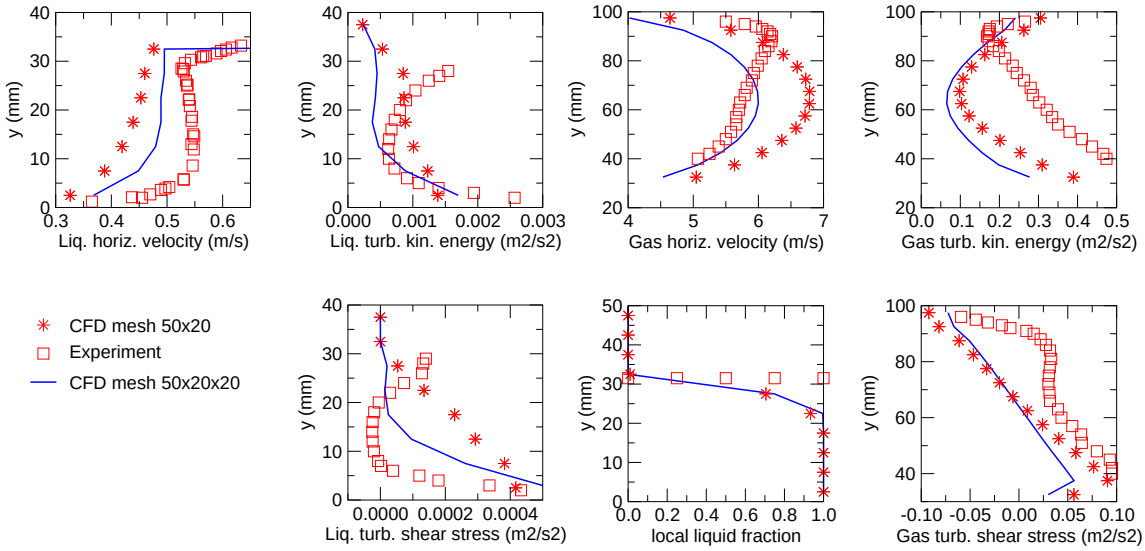

Fig. 4. Run 400 (wavy)- NEPTUNE_CFD calculation with large interface turbulence and friction models with a 2D mesh (50x20) (✳) and a 3D mesh (50x20x20) (—) versus measurements (□), 9.1 m from the inlet.

4.4 Discussion

The smooth regime is calculated in a satisfactory way. Therefore the run 250 will be used in the future mainly for non-regression checks.

The wavy case calculations are not satisfactory. Getting a good agreement in the wavy case is a difficult task. An obvious development, which is under way, is to include the friction due to the waves in the wall-type law used along the free surface. The problem then is the evaluation of the wave characteristics. The other problem is the important 3D recirculation which may call for a more precise turbulence modelling than k-ε. R_{ij}-ε model sensitivity may be tested in a first step.

This Fabre *et al.* (1987) experiment is very useful. It is currently assumed that measurements and boundary conditions uncertainties are negligible in comparison with CFD agreement. Data are available for future developments and improvements, which concern non isotropic turbulence or 3D flows in the wavy case.

5 HEAT AND MASS TRANSFER

5.1 Model

The important closure law for DCC is the heat transfer coefficient $h_{L,i}$ between the liquid and the interface. There are many models available since several decades (Theofanous *et al.*, 1976) (Banerjee, 1978) (Bankoff, 1980). In the early 2000's, our goal was to use a model suitable for CFD, which could predict the trends of COSI tests, which could be used in the reactor case without change, without arbitrary fitting constants. Then we could not select models validated on a 1D approach (averaging in pipes cross sections) or on smooth stratified flows or at low Reynolds numbers. We had to write a model which uses local variables available in the computations. This model was used in the SIMMER code (Coste, 2004) and is currently used in the NEPTUNE_CFD code (Coste *et al.*, 2008). It is written as follows in order to use k_l and ε_l calculated with the described above turbulence model:

$$h_{L,i} = \left(\rho_L C_{p,L} \lambda_L\right)^{\frac{1}{2}} \left(\frac{2}{3} k_L\right)^{\frac{1}{4}} \left(\frac{\upsilon^3}{\varepsilon_L}\right)^{-\frac{1}{8}} \tag{6}$$

$C_{p,L}$ is the specific heat and λ_L the thermal conductivity of liquid. Its form comes from the surface renewal model with a renewal frequency built with a Kolmogorov length and a turbulent velocity.

Recently, DNS and LES brought new insights and clarifications (Magnaudet and Calmet, 2006). DNS of Lakehal *et al.* (2007) showed that the surface divergence model of Banerjee *et al.* (2004) coming from the Hunt and Graham theory (1978) applies in the liquid phase. Some efforts are underway to position the $h_{L,i}$ NEPTUNE_CFD model with regard to them.

5.2 Validation on COSI

The COSI experiment was built to study PWR ECC injection in the cold leg during a LOCA. It was used in the CATHARE code condensation modelling studies (Janicot and Bestion, 1993). COSI represents a PWR cold leg with the safety injection at the scale of 1/100 for volume and power, and conservation of Froude number (Fig. 5). The downcomer is represented by a simple cylinder. Vapour is supplied to one of the extremities of the test section, the other being partially opened or closed, depending on the runs. A weir is located at the extremity of the pipe in some tests, before the downcomer, in order to set a water minimum level. The tests without weir correspond to a situation where the liquid level in the downcomer is lower than the cold leg junction with the downcomer. During the runs, which represent a LOCA, low temperature water (typically 20° to 80 °C) is injected in the cold leg which is usually filled with vapour at a pressure between about 2 and 7 MPa. The steady state runs are presently used for the analysis. Experimental values are averaged over a time period of 30 seconds. Measurements include temperature vertical profiles at eight sections of the cold leg and the condensation rate in the whole test section. A significant range of inlet vapour flow rates and safety injection flow rates is covered.

Therefore, depending also on the weir height, some phenomena may have a very different effect on measured temperature profiles from one run to the other, such as, for example: the cold water safety injection fall through the vapour; the entrainment of the jet by the vapour; the damping effect of thermal stratification on turbulence; the cold water impact on the cold leg wall. It is currently assumed that temperature measurements and boundary conditions uncertainties are negligible in comparison with CFD disagreement with measured temperatures. It makes COSI a fruitful validation experiment for a CFD approach to PTS.

The difficulty in the $h_{L,i}$ model validation on an experiment like COSI is that there may be compensations of errors: for example, a CFD overestimating turbulence and an $h_{L,i}$ underestimating the heat transfer for a correct turbulence input would give a correct heat transfer output. This weak point has been tentatively mitigated, not only by making calculations with same $h_{L,i}$ model covering a wide range of test parameters and mesh sizes (about sixteen COSI runs), but also by considering calculations with same $h_{L,i}$ model with two quite different CFD involving two quite different turbulence modelling.

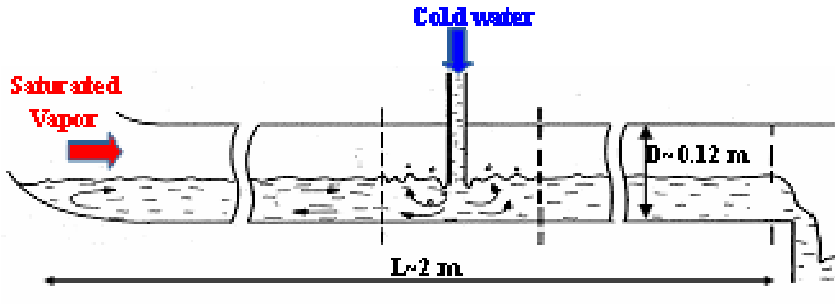

Fig. 5. Sketch of the flow in COSI tests.

The first CFD was 2D with some adaptations to take into account some 3D effects (Coste, 2004). It was done in SIMMER-III (Tobita *et al.*, 2006), a multi-phase finite volume code, with a staggered mesh and a second order spatial discretization of all transport equations. The typical mesh for the test section was structured and included 87 cells in horizontal direction and 18 cells in vertical direction. The approach included a special treatment for interfacial area and drag between liquid and vapour, in case of interfaces larger than cells size. The turbulence modelling was algebraic, using engineering relationships, originally used in single-phase flows, without change of original constants, including the thermal stratification effect via a Richardson number dependence.

The second CFD is 3D. It is done with the NEPTUNE_CFD code, with the approach described in this paper. An example of computational domain is shown in Fig. 6. The 3D calculations corresponding to the results of Fig. 8 have been performed with a quite large range of meshes sizes and refinement choices, as illustrated in Fig. 7. Fig. 8 left calculations have been performed typically with meshes like Fig. 7 left and middle. The "3D fine mesh" calculations of Fig. 8 right have been performed with the mesh of Fig. 7 right.

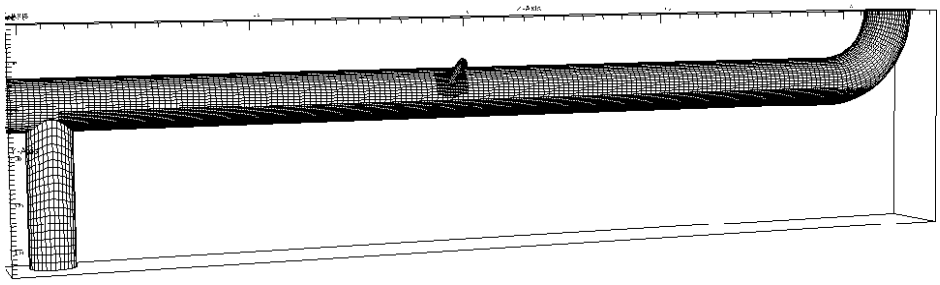

Fig. 6. Example of a NEPTUNE_CFD computational domain for a COSI test calculation

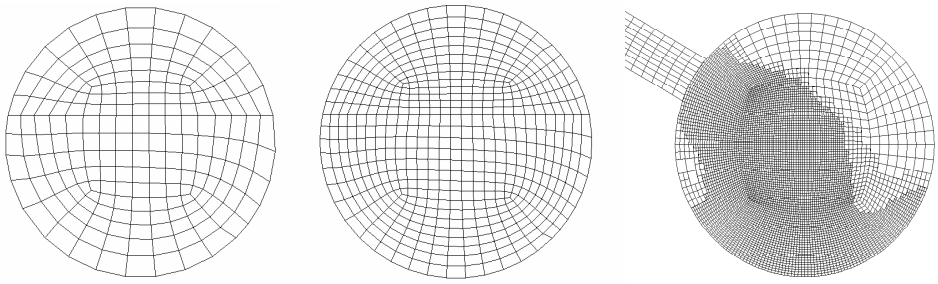

Fig. 7. Cross section in the plane containing the ECC axis of three examples of meshes (the ECC pipe is not shown on the left and middle figures for post-treatment reasons) used in NEPTUNE_CFD calculations: the corresponding mesh for the whole calculation includes, from left to right: 31700, 112000, 494000 cells.

Fig. 8 shows CFD results obtained with the two codes as described above, using in all cases $h_{L,i}$ model of Eq. (6), compared to experimental data. Fig. 8 left gives the calculations errors on condensation rate calculated as:

$$\frac{\delta\Gamma}{\Gamma} = \frac{\Gamma_{cond} - \Gamma_{\exp}}{\Gamma_{\exp}} \tag{7}$$

Γ_{exp} (resp. Γ_{cond}) is the measured (resp. calculated) condensation rate. Γ_{exp} is including some condensation in the downcomer, below the cold leg. It was estimated to be between 0 and 20% of the total condensation rate. On the other hand, as this condensation is technically difficult to represent in the calculations, Γ_{cond} is taken in the cold leg only. Therefore the condensation rate experimental uncertainty band in Fig. 8 left is between, approximately, -20% and 0%. The temperatures are measured on N_z =16 points in the vertical direction, at N_x =8 locations along the test section axis. Fig. 8 right gives the calculations errors on temperature calculated as:

$$\frac{\delta T}{T} = \frac{1}{N_z N_x} \sum_{i=1}^{N_x} \sum_{j=1}^{N_z} \left| \frac{T_{calc} - T_{\exp}}{T_{sat} - T_{SI}} \right| \tag{8}$$

T_{sat} (resp. T_{SI}) is the saturation (resp. safety injection) temperature. In the vertical direction, the cells in gas are not taken into account because the temperature there is not difficult to calculate (close to saturation). Only temperatures in the liquid pool cells are considered. The temperature experimental uncertainty can be assumed negligible in comparison with calculation/experiment disagreement.

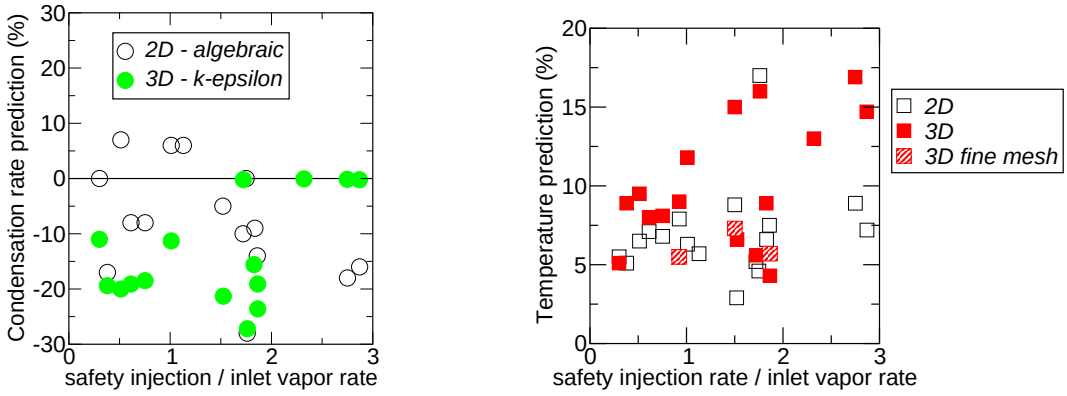

Fig. 8. Comparison with COSI experimental results of 2D (SIMMER-III, algebraic model for turbulence) and 3D (NEPTUNE_CFD, k-e model for turbulence) calculations with the same $h_{L,i}$ model (Eq. 2). On the left: condensation rate experimental uncertainty band is between -20% and 0%. On the right: temperature experimental uncertainty can be assumed negligible in comparison with calculations/experiment disagreements.

The calculations results summarized on Fig. 8 of runs with different boundary conditions and meshes show that some great tendencies of some main phenomena are taken into account by the $h_{L,i}$ model of Eq. (6). A certain level of confidence in NEPTUNE_CFD calculations can be deduced but some weak points spur on further investigations. Let us mention two of them. Firstly, even if calculations with fine meshes lead to reasonable results, it is still necessary to demonstrate on simple cases the behaviour of the present heat and mass transfer model as a function of cells size. Secondly, the same model is used in the jet region impact and far upstream or downstream, where the flow is stratified and the turbulence may be weaker. Here are two reasons to consider stratified steam water flow experiments.

5.3 Validation on a steam-water stratified flow

The LAOKOON experiment has been used within the European project NURESIM for CFD (Scheuerer *et al.*, 2007). The LAOKOON test cases (Hein *et al.*, 1995) relate to horizontal, stratified flow of sub-cooled water with condensation of saturated dry steam along the water surface. NEPTUNE_CFD reproduced the qualitative behaviour of the flow and energy field but the ECC water temperature in the bottom part of the channel was underestimated. A serious disadvantage of the test case was that the results for the temperature profiles and condensation rates were sensitive to variations of the inlet boundary conditions for the turbulence quantities which made model improvement difficult.

Lim *et al.* (1984) experiment also deals with interfacial condensation of a turbulent stratified steam-water flow in a rectangular cross section. Its dimensions are 0.0635 m high, 0.3048 wide, 1.601 m long. The inlet water height is 1.59 cm. There are five tests sections along the axis located at 0.15, 0.30, 0.59, 0.87, 1.23 m from the channel inlet. The two selected test cases are listed in Table 1. In run 1, the interface was smooth. In run 2, the interface was smooth from the channel inlet to 0.4 m, then switching to a wavy interface further off.

	Run 1	Run 2
Inlet steam mass flow rate (kg/s)	0.041	0.065
Inlet steam temperature (°C)	111	116
Inlet water mass flow rate (kg/s)	0.657	0.657
Inlet water temperature (°C)	25	25

Table 1: Experimental conditions of Lim *et al.* (1984)

Although further calculations, especially sensitivity to the mesh size and to boundary conditions, are absolutely necessary, four preliminary NEPTUNE_CFD calculations of Lim *et al.* experiment are presented in Fig. 9 because they may help to discuss the interest of Lim *et al.* experiment and the current context of PTS CFD. The Fig. 9 shows the steam mass flow rate as a function of the axial position in the channel, from the inlet. On left: run 1. On right: run 2. The NEPTUNE_CFD calculations have been performed both with $h_{L,i}$ model of Eq. (6) and with $h_{L,i}$ model based on Lakehal *et al.* (2007). It is clear, in the smooth regimes of run 1 in the whole channel and of run 2 until 0.4 m, that the Lakehal *et al.* (2007) model is correct whereas Eq. (6) largely overestimates the condensation. In the smooth regime, dynamic quantities, especially about turbulence, used as inputs in the $h_{L,i}$ model, should be relatively correct, considering Fig. 3. It is not clear after the smooth to wavy transition regime around 0.4 m of run 2 which model is correct, because there is not enough confidence in ca
Fi

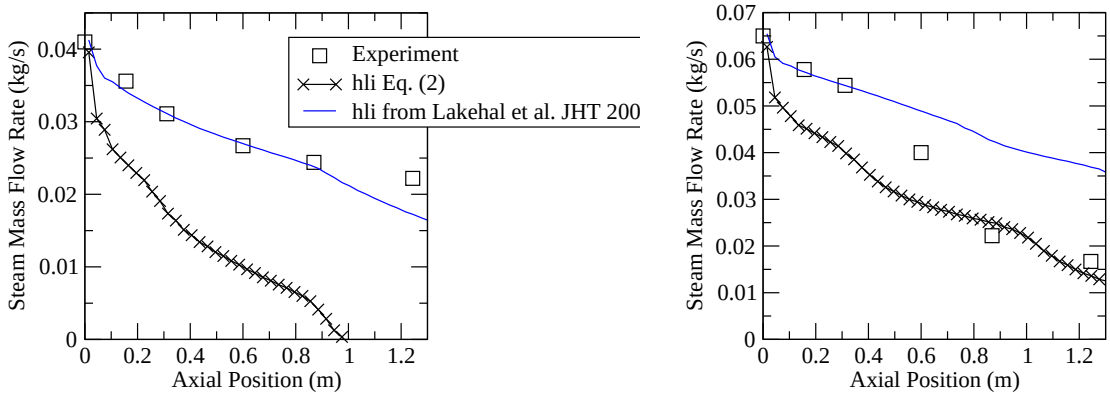

Fig. 9. Steam mass flow rates versus axial position from the inlet: comparison with Lim et al experiment of NEPTUNE_CFD preliminary calculations, with $h_{L,i}$ model of Eq. (6) and with $h_{L,i}$ model from Lakehal *et al.* (2007). On the left: run 1 (smooth interface). On the right: run 2 (smooth interface from axial position 0 to 0.4 m, wavy further off).

The Lim *et al.* experiment provides data that LAOKOON does not and vice versa. In LAOKOON, only the temperature vertical profiles and a global approximate condensation rate are available. In Lim *et al.*, there are no temperature vertical profiles, but vertical profiles of water and steam velocities, axial profiles of water thickness, steam pressure, steam flow rates and estimated heat transfer coefficients, are available. The distinction of two regimes, smooth and wavy, with a clear effect on the measurements, provides valuable data challenging for CFD.

6 CONCLUSION

The current PTS modelling used in NEPTUNE_CFD includes a large interface recognition algorithm, an approach of three cells layer thick of large interfaces and large interface specific models for friction, turbulence and heat transfer.

Fabre *et al.* (1987) air-water stratified flow experiment is useful to qualify friction and turbulence models in both smooth and wavy regimes. Current models are satisfactory in the smooth regime but not in the wavy one. An explanation is that the wall-type law used at the free surface to calculate the friction does not include yet a roughness to account for waves.

Lim *et al.* (1984) steam-water stratified flow experiment is useful to qualify the heat and mass transfer model once friction and turbulence models are qualified on Fabre *et al.* experiment. Preliminary calculations show that current friction and turbulence models are satisfactory in the smooth regime provided that Lakehal *et al.* (2007) model for the heat transfer on liquid side is used. The current liquid side heat transfer model (Coste, 2004) overestimates this heat transfer in this smooth regime. The wavy regime requires further investigations.

On the other hand, the (Coste, 2004) model has been successfully qualified on sixteen COSI tests which represent a cold leg scaled 1/100 for volume and power from a PWR under SBLOCA conditions. This difference of agreement between COSI and Lim *et al.* is presently explained by the flow regime difference, COSI being assumed not to be in a smooth regime. However, as COSI is a rather integral test, the whole set of PTS models is involved in calculations: so separate effect tests are necessary to acquire a better knowledge of each individual models behaviour. Those three experiments used in this paper are complementary and provide valuable data which can feed further validation and development of PTS CFD.

Future developments in the current PTS modelling will aim at improving the prediction of wavy Fabre *et al.* tests and of Lim *et al.* tests, while keeping at least current satisfactory results on COSI and on smooth runs of Fabre *et al.*.

ACKNOWLEDGMENTS

The authors are grateful to Alain Martin (EDF) and Dominique Bestion (CEA) for support and discussions. The NEPTUNE project is funded by EDF (Electricité de France), CEA (Commissariat à l'Energie Atomique), AREVA-NP and IRSN (Institut de Radioprotection et de Sûreté Nucléaire). The study has been partly carried out in the framework of the NURESIM project which is partly funded by the European Commission in the framework of the Sixth Framework Program (2004-2006).

REFERENCES

S. Banerjee, “A surface renewal model for interfacial heat and mass transfer in transient two-phase flow”, *Int. J. Multiphase Flow*, 4, 571–573, (1978).

S. Banerjee, D. Lakehal, M. Fulgosi, “Surface divergence models between turbulent streams”, *Int. J. Multiphase Flow*, 30, 963-977, (2004).

S.G. Bankoff, “Some condensation studies pertinent to LWR safety”, *Int. J. Multiphase Flow*, 6, 51-67 (1980).

P. Coste, “Computational simulation of multi-D liquid-vapor thermal shock with condensation”, *Proc. ICMF’04*, Yokohama, Japan, May 30- June 4 (2004).

P. Coste, J. Pouvreau, C. Morel, J. Laviéville, M. Boucker, A. Martin, "Modelling turbulence and friction around a large interface in a three-dimension two-velocity eulerian code", *Proc. NURETH 12*, Pittsburgh, USA, September 30- October 4 (2007).

P. Coste, J. Pouvreau, J. Laviéville, M. Boucker, "A two-phase CFD approach to the PTS problem evaluated on COSI experiment", *Proc. ICONE 16,* Orlando, USA, 11-15 mai (2008).

J. Fabre, L. Masbernat, C. Suzanne, "Stratified Flow, Part I: Local Structure", *Multiphase Science and Technology*, 3, 285-301 (1987).

M. Fulgosi, D. Lakehal, S. Banerjee, V. DeAngelis, "Turbulence in a sheared air-water flow with a deformable interface", *J. Fluid Mech*., 482, 319-345 (2003).

A. Guelfi, D. Bestion, M. Boucker, P. Boudier, P. Fillion, M. Grandotto, J.M. Hérard, E. Hervieu, P. Péturaud, "NEPTUNE - A New Software Platform for Advanced Nuclear Thermal-Hydraulics", *Nuclear Science and Engineering*, 156, pp. 281-324, 2007.

D. Hein, H. Ruile, J. Karl, "Kühlmittelerwärmung bei Direktkontaktkondensation an horizontalen Schichten und vertikalen Streifen zur Quantifizierung des druckbelasteten Thermoschocks", BMFT Forschungsvorhaben 1500906, Abschlußbericht, Lehrstuhl für Thermische Kraftanlagen, TU München, Germany (1995).

M. Ishii, "Thermo-fluid Dynamics Theory of Two-Phase Flow", Eyrolles, Paris, 1975.

A. Janicot, D. Bestion, "Condensation modelling for ECC injection", *Nuclear Engineering and Design*, 145, 37–45, (1993).

D. Lakehal, M. Fulgosi, G. Yadigaroglu, "Direct numerical simulation of condensing stratified flow", *ASME J. Heat Transfer*, 130, 021501 (2007).

J. Laviéville, P. Coste, "Numerical modelling of liquid-gas stratified flows using two-phase Eulerian approach", *Proc. 5th International Symposium on Finite Volumes for Complex Applications*, Aussois, France, June 08-13 (2008).

I.S. Lim, R.S. Tankin, M.C. Yuen, "Condensation measurement of horizontal cocurrent steam-water flow", *J. Heat Transfer*, 106, 425 (1984).

P. Liovic, D. Lakehal, "Multi-physics treatment in the vicinity of arbitrarily deformable gas liquid interfaces", *J. Comp. Phys*., 222, 504-535 (2007).

D. Lucas, D. Bestion, E. Bodèle, M. Scheuerer, F. D'Auria, D. Mazzini, B. Smith, I. Tiselj, A. Martin, D. Lakehal, J.-M. Seynhaeve, R. Kyrki-Rajamäki, M. Ilvonen, J. Macek, "On the simulation of two-phase flow Pressurized Thermal Shock (PTS)", *Proc. NURETH 12*, Pittsburgh, USA, September 30- October 4 (2007).

J. Magnaudet, I. Calmet, "Turbulent mass transfer through a flat shear-free surface", *J. Fluid Mech*., 553, 155-185 (2006).

N. Méchitoua, M. Boucker, J. Laviéville, J.M. Hérard, S. Pigny, G. Serre, "An unstructured finite volume solver for two-phase water/vapor flows modelling based on an elliptic-oriented fractional step method", *Proc. NURETH-10*, Seoul, Korea, 5-9 October (2003).

R. Nagasoa, "Direct numerical simulation of vortex structures and turbulent scalar transfer across a free surface in a fully developed turbulence", *Phys. Fluids*, 11, 1581-1595 (1999).

M. Scheuerer *et al.*, "Numerical simulation of free surface flows with heat and mass transfer", *Proc. NURETH-12*, Pittsburgh, USA, September 30 -October 4 (2007).

T.G. Theofanous, R.N. Houze, L.K. Brumfield, "Turbulent mass transfer at free, gas-liquid interfaces, with applications to open-channel, bubble and jet flows", *Int. J. Heat Mass Transfer*, 19, 613-624 (1976).

Y. Tobita, Sa. Kondo, K. Morita, W. Maschek, P. Coste, T. Cadiou, "The development of SIMMER-III, an advanced computer program for LMFR safety analysis, and its application to sodium experiments", *J. Nuclear Technology*, 153, pp.245-255 (2006).

E.R. Van Driest, "On turbulent flow near a wall", *J. Aeronautical sciences*, 23 (1956).

W. Yao, D. Bestion, P. Coste, M. Boucker, "A three-dimensional two-fluid modelling of stratified flow with condensation for pressurized thermal shock investigations", *J. Nuclear Technology*, 152, 129-142 (2005).